EXPERIMENTAL STUDIES ON UNSTEADY AERODYNAMIC LOSS OF A HIGH-PRESSURE TURBINE CASCADE

Ken-ichi Funazaki and Yoshinori Sasaki
Department of Mechanical Engineering
Iwate University
Morioka, Japan

Tadashi Tanuma
Heavy Apparatus Engineering Laboratory
Toshiba Corporation
Yokohama, Japan

ABSTRACT

The objective of this study is to investigate how the wake passage impacts the aerodynamic performance of turbine rotor blades in turbomachines. Despite a number of research activities, information on aerodynamic loss generation in turbine rotors under the influence of unsteady flows encountered in actual turbomachines is still limited. This paper describes our newly started research project which aims to gain insight into the physics of the aerodynamic interaction between turbine rotors and incoming periodic wakes, and to establish a method for evaluation of unsteady aerodynamic losses of turbine rotors generated by the wakes. In this study, using a linear turbine cascade and a wake generator, the wake-affected flow field upstream and downstream of the cascade is measured in detail with a five-hole pneumatic pressure tube and a hot-wire probe in order to obtain time-averaged as well as time-resolved characteristics of the flow field. It is accordingly found that the wake passing affects the flow field around the turbine cascade, which yields considerable change in the two-dimensional cascade loss as well as in the secondary vortex structure. Moreover, it is also revealed that a so-called negative jet effect associated with the wakes plays an important role in unsteady loss generation of the turbine cascade, which is in contradiction to the findings by Hodson and Dawes (1996).

NOMENCLATURE

C_d	: drag coefficient of a wake generating bar
C_p	: pressure coefficient ($=(P_T-p)/(P_T-p_{in})$)
C_x	: axial chord length
d	: diameter of a wake generating bar
e_1, e_2	: signals from the hot-wire probe
f	: bar-passing frequency ($=nn_c/60$)
H	: blade height
h_0	: stagnation enthalpy
n	: number of cylinders used
n_c	: rotation number
P	: blade pitch
P_T	: stagnation pressure
ΔP_T	: stagnation pressure loss associated with the wake generating bars
p	: static pressure
Re	: Reynolds number ($= U_{in}C_x/\nu$)
S	: Strouhal number ($= fC_x/U_{in}$)
s	: bar or nozzle vane spacing
Tu	: turbulence intensity
t	: time
U_b	: moving speed of the bar at the radius 395 mm
U_{in}	: inlet velocity
$\tilde{v}(t_j)$	: ensemble-averaged velocity
$v_i(t_j)$	: sampled instantaneous velocity data
x,y,z	: axial, tangential and spanwise coordinates
α	: sensor angle with the flow direction
β_{in}	: inlet flow angle
ϕ	: flow coefficient ($= U_{in}\cos\beta_{in}/U_b$)
ρ	: density
ν	: kinematic viscosity
ζ	: stagnation pressure loss coefficient
ζ_{in}	: pitchwise-averaged stagnation pressure loss at the inlet of the cascade.

subscript

in, out	: inlet condition, outlet condition

INTRODUCTION

It is widely recognized that wakes from upstream blade rows greatly affects the flow structures around the subsequent blades and vanes in turbomachines, resulting in early boundary-layer transition over the blade surface, undesirable effects such as blade vibration, noise generation. Accordingly a number of studies have been made in the past to understand this very complicated phenomena. A very comprehensive survey on unsteady flow in turbomachines, including

Presented at the International Gas Turbine & Aeroengine Congress & Exhibition
Orlando, Florida — June 2–June 5, 1997

the wake interaction problem, was presented by Greitzer (1985). Afterward several excellent works were conducted by Gallus (1991) and his group, where they investigated unsteady flow field in an 1-1/2 stage turbine or a single compressor stage in great detail by use of LDV or triple-hot-wire probe. Yamamoto et al. (1993)(1994) executed similar studies, with special emphasis on the effects of blade-wake interaction upon secondary vortices or cooling air injected. Those studies clearly revealed complicated structure of unsteady flows in turbomachines. Funazaki and Nishiyama (1989) made extensive studies on wake-cascade interaction phenomena in a subsonic wind tunnel by use of a belt-driven cylinders as wake generator. They measured unsteady total pressures at the downstream of the cascade, comparing those data with their numerical predictions. Ladwig and Fotter (1993), using stationary bars as wake generator, investigated the influence of incoming wakes on the loss of a linear turbine cascade. Despite those efforts, however, satisfactory understanding of the flow is still beyond our scope. Especially, information is seriously lacking on how to evaluate unsteady loss of the blade row, which is strongly needed for aerodynamicists of turbomachines. Some numerical attempts were also made to predict blade profile loss under the influence of the wake passing, which did not yield satisfactory results though (Halstead et al. (1995)).

Recently, Curtis et al. (1996) have made an experimental study to measure unsteady profile losses of turbine blades under the influence of upstream passing wakes in a low-speed wind tunnel. Then Hodson and Dawes (1996) have presented an interpretation of those experimental data, taking account of the effect of fluctuating static pressures on the stagnation enthalpy. These studies are excellent ones concerning the loss generation in the cascade under the influence of the wake passing, which provides a basis for further discussions on these topics. However, the present authors feel great necessity for additional re-examination of their experimental findings or their interpretations for the purpose of better understanding of the wake-blade interaction phenomena as well as the loss generation mechanism in cascades subjected to the unsteady flow.

This study performs loss measurements for a linear cascade of high pressure turbine blades under the influence of periodically passing wakes generated from a spoked-wheel type wake generator similar to the one used in the previous study by Funazaki et al. (1996). Instead of a fast-response pressure tube, a conventional five-hole yawmeter is employed in this study to measure *time-averaged* loss distributions

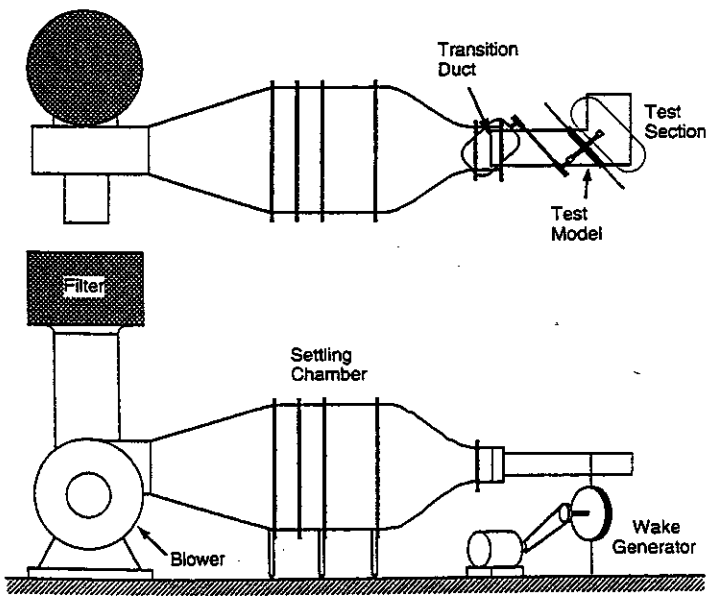

Figure 1 Test apparatus

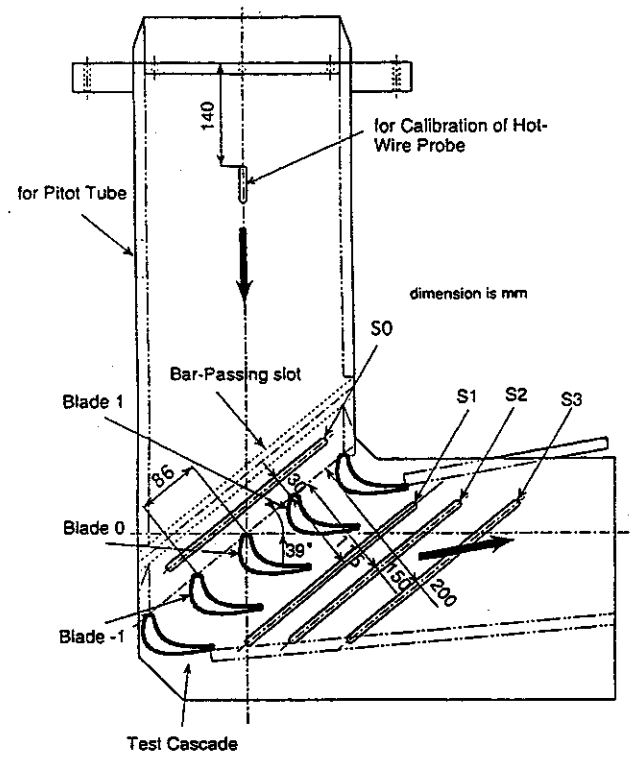

Figure 2 Configuration of the test cascade and the locations of aerodynamic measurements

Table 1 Cascade data and the flow condition

	Test Cascade	Real Turbine
Rotational Speed n [rpm]	1200	15000
Blade Chord C_x [m]	0.1	0.025
Static Temperature [K]	288	1450
Inlet Mach Number M	0.10	0.38
Reynolds Number Re	2.3×10^5	6.5×10^5
Pitch Ratio[1] s/C_x	0.21 (*)	0.57
Strouhal Number S	0.34	0.83
Nozzle Exit Angle [deg]	66	70
Inlet Flow Angle [deg]	39	39
Outlet Flow Angle [deg]	-61	-61

(*) bar number is 6, where the pitch is defined at the radius 395 mm (See Figure 3)

downstream of the moving bars as well as downstream of the cascade. Furthermore, a hot-wire probe is also used to measure the instantaneous flow field that is being affected by the wake passage. It is confirmed again in this study that a negative jet effect of incoming wakes plays an important role in the re-distribution process of the loss associated with the bar wakes. It is also verified that the incoming wakes greatly affects the secondary vortices of the cascade.

TEST APPARATUS

Figure 1 shows a schematic layout of the test apparatus used in this study. It resembles the one used in the previous study (Funazaki et al. (1996)), adopting a spoke-wheel type wake generator to simulate wakes from upstream stator vanes. Air from the blower, passing through the settling chamber and the contraction nozzle with the exit cross section of 250 mm height and 350 mm width, entered the test duct with the cross section of 130 mm x 266 mm. Figure 2 presents details of the test section and the test cascade used. The test cascade consisted of five identical blades. The blade chord length C_x and blade height H were 100 mm and 128 mm, respectively. The blade section was typical high pressure turbine blade. The cascade configuration and its flow conditions are listed in Table 1, accompanied by the data of the corresponding real turbine blades. Urethane-foam sheets with the shape of the blade section were attached to all the blade tips as sealant, so that any leakage from the tip clearance was completely avoided.

The spoked-wheel type wake generator, shown in Figure 3, consisted of a brass-made disk of 400 mm diameter and 6 or 12 circular cylinders of 250 mm length and 5 mm diameter on the disk rim. As mentioned above, the test cascade was based on high pressure

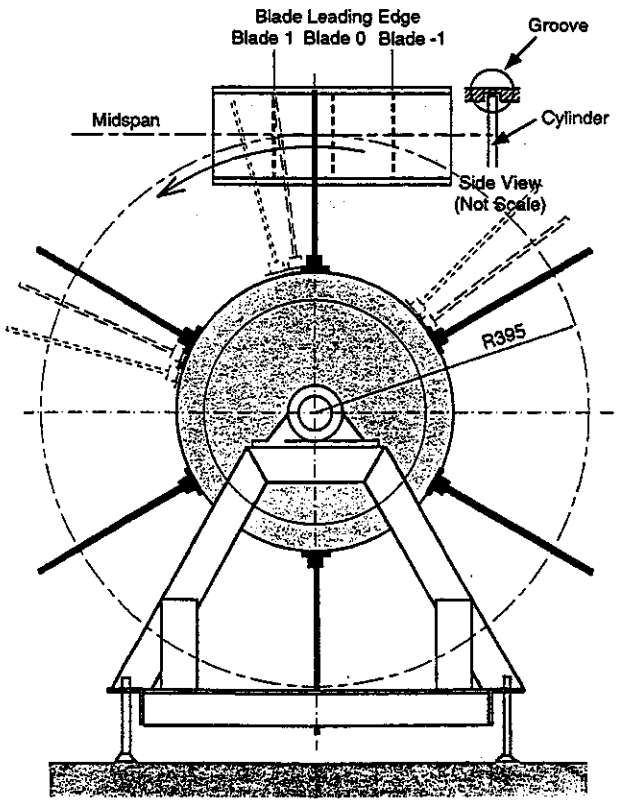

Figure 3 Front views of the wake generator and the cascade

turbine blades that required a relatively high inlet Reynolds number for emulation of the actual flow field. Restriction on the blade size available for the present test accordingly necessitated a large inlet velocity, although the required high Reynolds number could not be achieved in the present study at last as shown in Table 1. This high inlet velocity implied that the wake generator had to rotate with considerable speed in order to achieve a realistic velocity triangle for the cascade. The wake generator used in this study provided the required high rotational speed without any difficulty, however, it had a drawback in its wake structure, because it inevitably produced three-dimensional wakes to the test cascade of two-dimensional geometry, as schematically depicted in Figure 3. This was in contrast to the study by Curtis et al. (1996), where belt-driven moving bars generated two-dimensional wakes. To obtain two-dimensional impingement of the wakes at least against the center blade (Blade 0) in the cascade, the wake generator was positioned so that the vertical center line of the wake generator and the leading edge line of Blade 0 were aligned on the duct center plane.

The wake-generating bars on the wake generator moved in the plane located at $x/C_x = -0.63$, where x is the coordinate in the axial direction of the cascade. Openings through which the moving bars could pass were provided at the side and lower plates of the test duct, while the upper plate was only grooved to minimize the tip effect of the moving bars. Since these openings also worked as air bleed, the boundary layer development over the side and the lower plates of the duct was considerably suppressed, however, it was not the case for the boundary layer over the upper plate. Therefore, as described later, the boundary layer at the upper side of the cascade was considerably thicker than that of the lower side of the cascade. The peak turbulence intensity TI_{peak} and normalized wake width (W_{TI}/d) associated with the turbulence intensity profile for the present case were estimated at the locus of the blade leading edge, using experimental findings on wake characteristics given by Halstead et al. (1995). It was found in the present case that TI_{peak} normalized by cascade inlet velocity U_{in} was about 12 % and W_{TI} observed in the stationary frame of reference was about 70 mm, which dominated 17 % of the pitch of the wake generating bars at the radius 395 mm (Refer to Appendix of Halstead et al. (1995) for the relevant data of the wake characteristics). These values of the wake characteristics do not seem to be unusual ones for high pressure turbine stages (Dring et al. (1987)). Free-stream turbulence intensity attained was at a low level (less than 0.5 %).

MEASUREMENT TECHNIQUES

Pneumatic 5-hole yawmeter

A conventional pneumatic five-hole yawmeter as shown in Figure

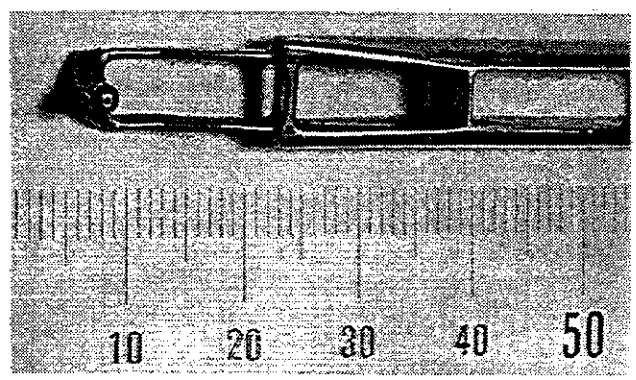

Figure 4 Pneumatic 5-hole yawmeter used in the measurement

4 was employed to measure time-averaged flow fields downstream of the moving bars as well as downstream of the turbine cascade. This probe, designed by Toshiba Co., was frequently used for the performance test of steam turbines. The probe was calibrated in the calibration wind-tunnel in Iwate University. It contained a sensing head with small diameter and a large opening was provided above the head to minimize its blockage effect. The yawmeter was traversed by use of a 3-axis traversing unit at the measurement slots of x/C_x = -0.3 (almost at the middle of the spacing between the moving bar and the blade leading edge), 1.15, 1.5 and 2. For convenience, these locations are referred to as Slot 0, Slot 1, Slot 2 and Slot 3, respectively (S0, S1, S2 and S3 in Figure 2). When the probe traverse was being carried out, the slot concerned was filled with a custom-tailored plug that made it possible for the probe to move smoothly with minimal air leakage, and the other slots were completely plugged. The pressure measurement was made using five differential-type pressure transducers and a PC-controlled datalogger.

A question may arise on how accurate this pneumatic probe can measure the pressure associated with the fluctuating flow due to the wake passage. A related discussion was made by Schulte and Hodson (1996), where they derived an expression for the stagnation pressure loss across the moving bars and compared the loss estimation with the experimental data. They claimed that the theoretical value had to be adopted instead of experimental data as the loss associated with the moving bars, unless the measurements were taken far downstream of the bars. Application of their expression (Eq. (A1) of Shulte and Hodson (1996)) for the present case predicted the stagnation pressure loss ΔP_T as,

$$\Delta P_T \Big/ \frac{\rho}{2} U_{in}^2 \cong 0.069 \ , \qquad (1)$$

where the values used were s/d=82.7, inlet flow angle $\beta_{in} = -39°$ (according to their notation), C_d=1.1 and the flow coefficient ϕ=0.55, while s/d=67, $\beta_{in} = -30.46°$, C_d=1.0 and ϕ=0.7 in the study of Shulte and Hodson. The value of the drag coefficient in the present case was determined taking account of the fact that the inlet Reynolds number based on the bar diameter in the relative frame of reference was 1.6×10^4 (see Schlichting (1979)). As described later, this predicted values happened to match the experimental data. Note that x_{bp}/d, axial distance between the probe and the moving bars normalized by the bar diameter, was 6.6. One might notice that the present result is somewhat conflicting with the findings by Shulte and Hodson (1996), which stated that x_{bp}/d less than 120 led to considerable measurement error in the stagnation pressure loss. The authors think this difference can be partially attributed to the relatively low Strouhal number (S =0.34) or the low amplitude of the pressure fluctuation in the present experiment. Another possible reason for this conflicting result might be the difference in the probe type used for the measurement of the stagnation pressure, i.e., the 5-hole yawmeter for the present case and conventional Pitot tubes for Shulte and Hodson case.

Hot-Wire Probe

A single hot-wire probe, which had a good frequency response up to 100 kHz, was used mainly to measure time-variant yaw angle at the blade mid-span behind the moving bars as well as behind the turbine cascade. The probe also yielded the time-resolved turbulent structure of the wake-disturbed flow field around the turbine cascade.

A measurement technique developed by Fujita and Kovasznay (1968) was employed to measure ensemble-averaged quantities with a single-wire probe. After setting the wire normal to a specified direction, velocity measurements were executed with the probe rotated by ±45° from the initial position. The data acquisition was always synchronized with the revolution of the wake generator, which guaranteed the multiposition measurement to be used for determining time-resolved (or ensemble-averaged) yaw angle. In principle, it was impossible to measure time-variant turbulent structure of the flow precisely by the multiposition technique, however, a method was introduced to evaluate *quasi* turbulence intensity for understanding of the wake-disturbed flow field more vividly. A two-axis traverse unit was used for the probe positioning.

DATA PROCESSING

Stagnation Pressure Loss

Stagnation pressure and yaw/pitch angle of the flow were calculated from the pressure data obtained by the 5-hole probe, using the calibration curves determined by Matsubara (1993). Stagnation pressure loss coefficients at the downstream of the wake generating bars as well as downstream of the cascade were defined as,

$$\zeta_{in}(z) = \left(P_{Tin} - \overline{P}_{T0}(z)\right) \Big/ \frac{1}{2}\rho U_{in}^2 \ , \qquad (2)$$

$$\zeta(y,z) = \left(\overline{P}_{T0}(z) - P_{T1}(y,z)\right) \Big/ \frac{1}{2}\rho U_{in}^2 \ , \qquad (3)$$

where P_{Tin}: inlet stagnation pressure, $\overline{P}_{T0}(z)$: pitchwisely mass-averaged stagnation pressure behind the moving bars (at Slot 0), $P_{T1}(y,z)$: local stagnation pressure measured at the downstream of the cascade (Slot 1).

Unsteady Velocity and Turbulence Intensity

As described above, the multiposition technique of a single hot-wire probe provided two-dimensional unsteady velocity influenced by the bar wake passage. The velocity components were calculated by the following relationship (Bruun, 1975),

$$\tilde{U}_x(t_j) = \frac{\tilde{e}_1(t_j) + \tilde{e}_2(t_j)}{2(\cos^2\alpha + k^2\sin^2\alpha)^{0.5}} \ , \qquad (4)$$

$$\tilde{U}_y(t_j) = \frac{\tilde{e}_2(t_j) - \tilde{e}_1(t_j)}{2A\tan\alpha\left(\cos^2\alpha + k^2\sin^2\alpha\right)^{0.5}} \ , \qquad (5)$$

$$A = \frac{\cos^2\alpha(1-k^2)}{\cos^2\alpha(1-k^2)+k^2} \ ,$$

$$\tilde{U}(t_j) = \sqrt{\tilde{U}_x(t_j)^2 + \tilde{U}_y(t_j)^2} \qquad (6)$$

where the subscript x represents a specified direction, which was normally aligned with the design exit flow angle, and the subscript y represents the direction perpendicular to the x-direction. The sensor angle α was set to be $\pi/4$ in this study. The value of k was empirically determined (=0.3). The quantities with $\tilde{}$ mean ensemble-averaged values, which was given by, for example,

$$\tilde{e}_1(t_j) = \frac{1}{m}\sum_{l=1}^{m} e_{1,l}(t_j), \ m = 100 . \qquad (7)$$

Since turbulence statistics could not be exactly calculated due to the multiposition technique used, a quasi turbulence intensity was introduced for convenience to envision the wake-affected unsteady flow field, which was defined as follows,

$$Tu(t_j) = \frac{1}{U_{in}} \sqrt{\frac{1}{m-1} \sum_{l=1}^{m} \left(\tilde{U}(t_j) - U_l(t_j) \right)^2}, \qquad (8)$$

where $U_l(t_j)$ was an unsteady velocity calculated by substituting sampled instantaneous data into Eqs. (4)(5) and (6) instead of the corresponding ensemble-averaged data.

Uncertainty Analysis

Precision of the differential-type pressure transducers used was about ±5[Pa] and the error associated with the data logging was about ±2 [Pa], which followed that the uncertainty of the stagnation pressure loss was about ±1.5 % of the inlet dynamic pressure.

RESULTS

Static Pressure Distribution

The static pressure distribution over the blade surface was numerically determined by use of a potential flow analysis code because there were no test blades provided with pressure taps in the present study. The accuracy of this code was already checked with several experiments. Calculated pressure distribution C_p is shown in Figure

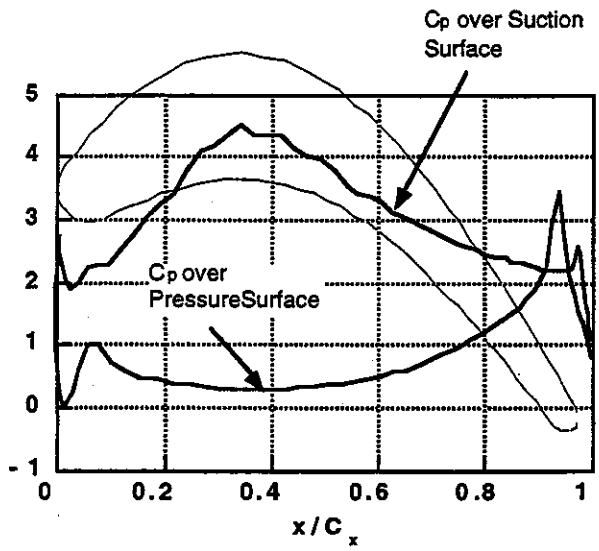

Figure 5 Calculated distribution of static pressure coefficient over the test blade surface

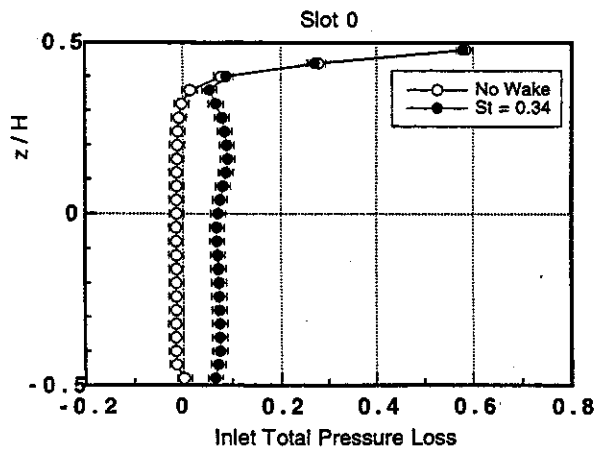

Figure 6 Spanwise distributions of the inlet stagnation pressure loss with and without the incoming wakes

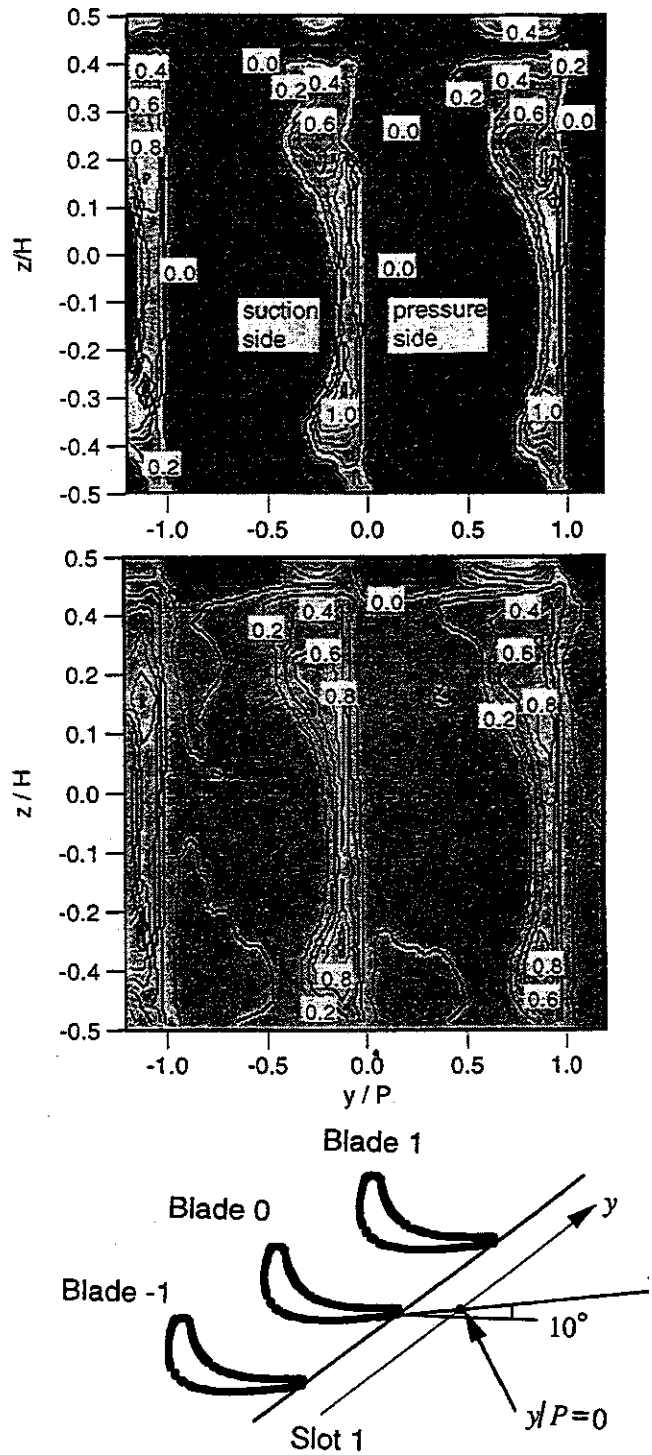

Figure 7 Stagnation pressure loss contours measured with the pnuematic pressure tube at Slot 1 (upper) with no wakes (lower) with wakes

5, accompanied with the blade section profile. There appears a adverse pressure gradient after x/C_x=0.4 on the suction surface. As shown later, flow visualizations confirmed a separation bubble around there.

Stagnation Pressure Loss across the Moving Bars

Figure 6 displays the pitchwise-averaged stagnation loss coefficient $\zeta_{in}(z)$ with and without the influence of the incoming wakes. Since there was no bleeding slot on the upper plate of the test duct,

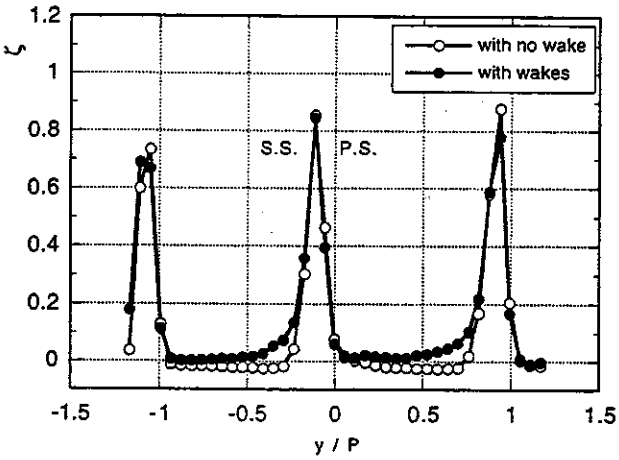

Figure 8 A comparison between the stagnation pressure losses for the cases with wakes and with no wakes at Slot 1, the data being radially averaged over the midsan region

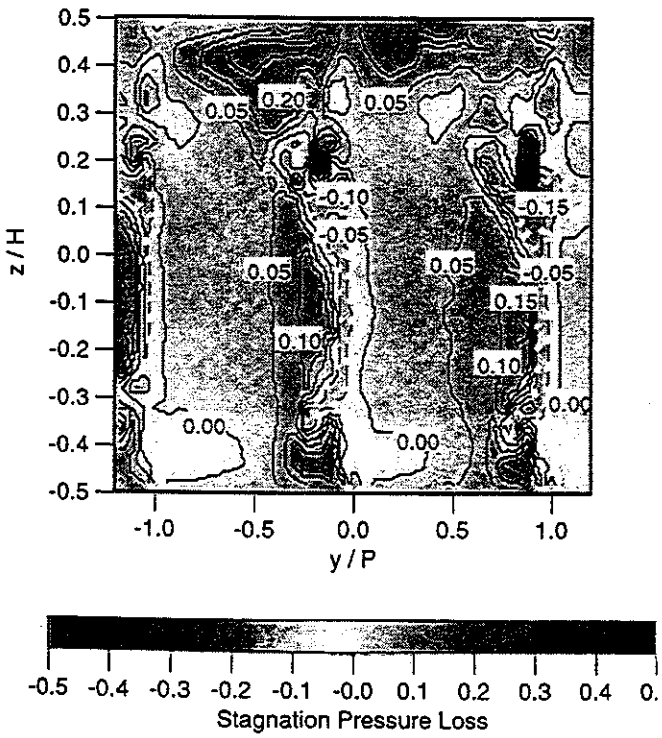

Figure 9 Difference in stagnation pressure loss between the cases with wakes and with no wakes at Slot 1 (+ : increase / - : decrease)

the boundary layer at the blade tip side was considerably thick compared with that of the hub side, and the associated loss was accordingly large. Except for the tip region, stagnation pressure loss occurred across the wake generator and its value was about 0.07, which almost agreed with the calculation shown in Eq. (1). One might notice that the stagnation pressure loss profile exhibits a slight increase toward the tip, followed by gradual decrease. This was probably due to the three-dimensionality of the incoming wakes or effects of the thickened boundary layer at the tip side. Therefore, the following discussion is restricted mainly to the flow events observed at the area below $z/H \equiv 0.3$.

Stagnation Pressure Loss downstream of the Cascade

Figure 7 shows stagnation pressure loss contours measured over the traverse plane at Slot 1 with and without the existence of the bar wakes, where Slot 1 was 15% axial chord distant from the trailing edge of the cascade. Also shown is the explanatory figure of the coordinate system downstream of the cascade, where $y/P = 0$ is the intersection between the y-coordinate and the line extended from the trailing edge of Blade 0 in the direction of the design exit flow. Recall that the present definition (Eq. (3)) measured the cascade loss on the basis of the difference between the pitchwise-averaged stagnation pressure at the inlet of the cascade and the local stagnation pressure at the downstream of the cascade for both cases with and without bar wakes. It does not appear that the loss contours drastically changed due to the wake passing, however, the background loss observed between the two neighboring blade wakes increased by 0.05 on average. Figure 8 provides a comparison between the pitchwise distributions of the stagnation pressure loss coefficients for the no wake and the wake conditions, where these distributions were calculated by averaging several pitchwise data measured near the midspan region where the flow was seemingly two-dimensional. Slightly negative values is observed for the no wake case, which could be due to the error associated with the pressure measurement as mentioned above. It is evident from this figure that the stagnation pressure loss gradually increased towards the suction side of the blade wake. This situation becomes much clearer in Figure 9. This figure was obtained by subtracting the loss distribution with no influence of the bar-wake passage (Figure 7 (upper)) from the bar-wake-affected loss distribution (Figure 7 (lower)). Note that a region bounded by a solid line or a broken line corresponds to the region with positive or negative value, representing a relative increase or decrease in stagnation pressure loss due to the bar-wake passage. It was confirmed that relatively high loss regions tends to cluster near the suction side of the blade wakes at the midspan.

Figure 9 also reveals the appearance of the regions with slightly negative value at the locations of the blade wakes, which means that the stagnation pressure loss associated with the blade wake (or blade profile loss) was more or less reduced by the passage of the bar-wakes. As Hodson (1990) described, wake passage over a blade surface leads to an increase in the blade profile loss. This was also observed by the experiment done by Funazaki and Tanuma (1996). A question was raised on why the blade loss decreased, rather than increased, even under the influence of the wakes. A flow visualization by means of oil flow technique was therefore conducted to find out the reason. Figure 10 shows oil-flow patterns over the blade suction surface with and without the incoming wakes, where the blade was exposed to the flow about for 5 minutes in both cases. In the no wake case, there appeared accumulated oil around the throat region, indicating the existence of a separation bubble around there. On the other hand, after exposing the blade to the flow including incoming bar wakes,

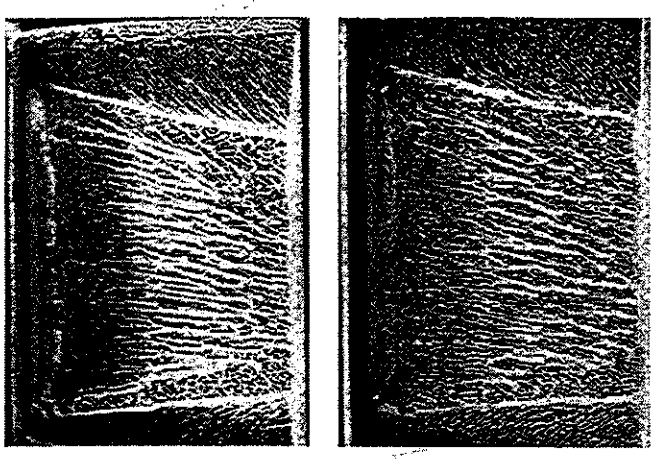

Figure 10 Oil flow patterns on the blade suction surface (left) with no wakes (right) with wakes

the separation bubble almost diminished, probably due to a direct effect of the wake turbulence and/or an indirect effect of the wake-induced transitional boundary layer prior to the separation bubble. From these observations it can be concluded that the increase in boundary layer loss due to the wakes was considerably compensated by the loss reduction caused by the suppression of the separation bubble over the blade suction surface, resulting in the observed decrease in stagnation pressure loss within the blade wakes. Similar findings were already reported by Schutle and Hodson (1996), where they confirmed a reduction in stagnation pressure loss by the incoming wakes at a relatively low Reynolds number case in which a separation bubble occurred on the suction surface.

Effects of the Wake Passage upon Secondary Flows

The five-hole yawmeter used in this study made it possible to see some effects of the bar-wake passing upon the secondary flow development, although it was not intended initially. Figure 11 shows the secondary flow fields for cases with and without incoming bar wakes. Note that a secondary velocity vector at an arbitrary position in Figure 11 was calculated in a simple manner by subtracting the velocity measured at a point on the traverse plane from the velocity measured at the midspan at the same y/P as the point in question, then projecting the difference onto the traverse plane. These two figures clearly indicate that the incoming wakes considerably affected the passage vortices developed within the blade-to-blade passage, seemingly reducing the strength of the passage vortices, especially at the tip side of the blades. Close inspections of the wake-affected oil-flow patterns of Figure 10 (the right photograph) exhibits somewhat unclear traces of the lift-off lines compared to those of the no wake condition. This also supports the above finding.

Time-Resolved Velocity Distributions

Hot-wire probe measurements were conducted over the entire traverse planes. It was consequently found that the contours of the time-averaged streamwise velocity calculated from the unsteady velocity data almost agreed with those obtained with the pneumatic probe, although the hot-wire probe used was not suitable for such a three-dimensional measurement. By checking several time-averaged velocity data, it appeared that the time-resolved velocity data measured at the midspan were practically free from the three-dimensionality of the flow field at least on the traverse plane at Slot 1. Thus in the

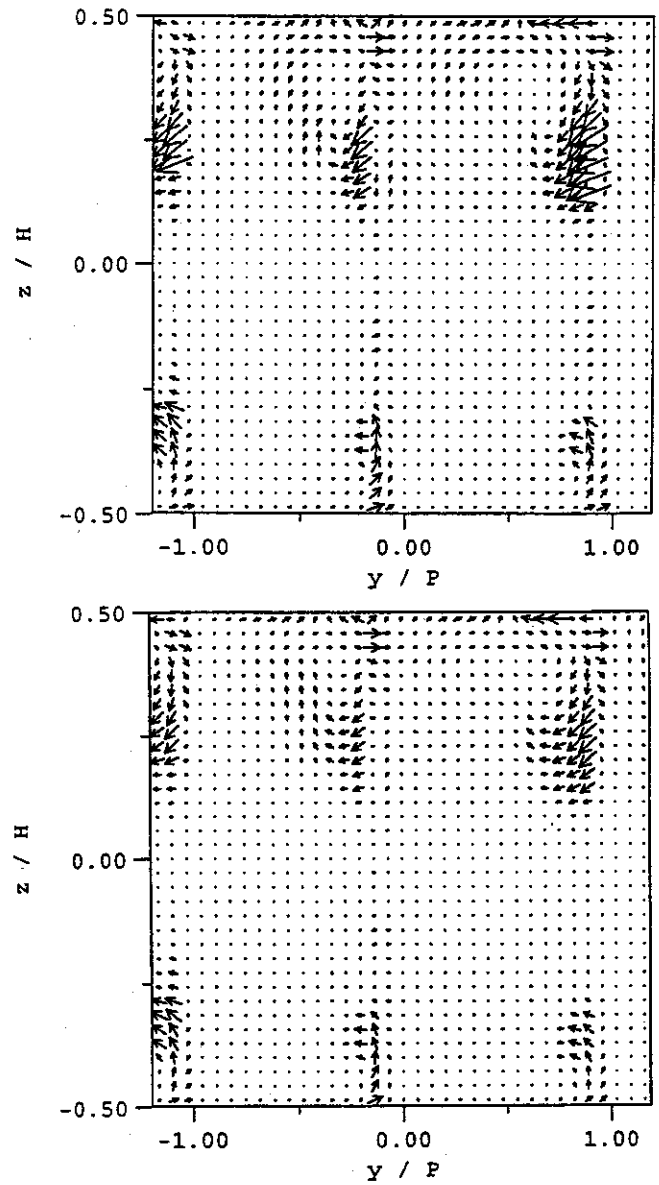

Figure 11 Secondary flow vectors at Slot 1 (upper) with no wakes (lower) with wakes

following we concentrate our concern on the time-resolved velocity data measured at the blade midspan.

Figures 12 and 13 are the contours on the distance-time diagrams representing the magnitude and the yaw-angle of the time-resolved velocity along the midspan at Slot 1, where the abscissa of the diagram represents the elapse time from the onset of the measurement and the ordinate is the pitchwise distance extending from Blade -1 to Blade 1. In order to clarify the effect of the wake passing, the data obtained at the no wake condition were subtracted from those with the influence of the wake passing. Note that these figures depict the contours around the blade wake downstream of Blade 0. The velocity was normalized with the inlet velocity U_{in} and the yaw angle was positive in the direction to Blade 1. In Figure 12 solid lines, in conjunction with the dark-shaded region, represent increases in the velocity relative to the no wake condition, while broken lines and the light regions represent

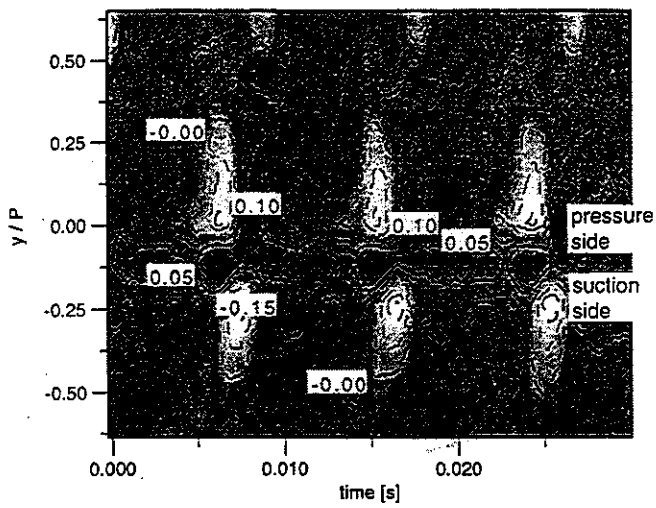

Figure 12 Contours of the magnitude of time-resolved velocity on the distance-time diagram (blade midpan at Slot 1)

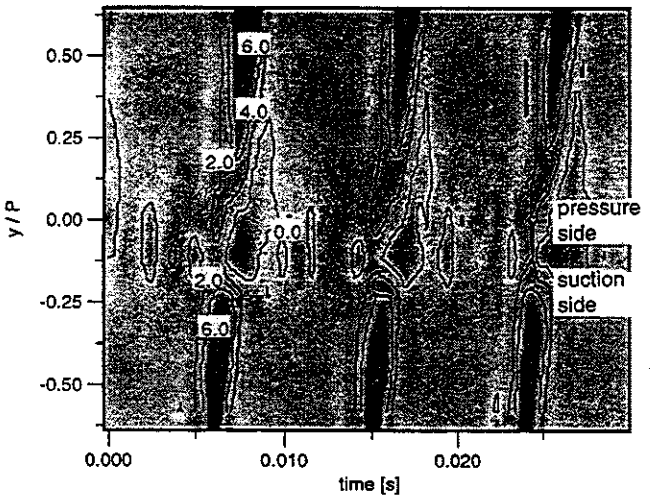

Figure 13 Contours of the yaw-angle of time-resolved velocity on the distance-time diagram (blade midpan at Slot 1)

the decrease in the velocity. This figure shows that the magnitude of the time-resolved velocity on the suction side of the blade wake became smaller than that of the no wake condition as a whole. In contrast, the flow velocity on the pressure side exhibited a sinusoidal change in magnitude, that is, a periodic decrease followed by an increase. It can be stated that these time-varying magnitude of the velocity is due to the effect of the negative jet. Besides, one may find rapid increase in velocity inside the blade wake, on which no further information is available.

As shown in Figure 13, the wake passage caused an increase in the yaw angle outside the blade wake, while the bar wake passage was less prominent inside the blade wake. Apparently there arose a pitchwise variation of the yaw angle, It appears that the yaw angle tended to increase near the suction side of the blade wake and decrease near the pressure side. Similar results were obtained at the further downstream slot from the cascade. Theses phenomena were due to

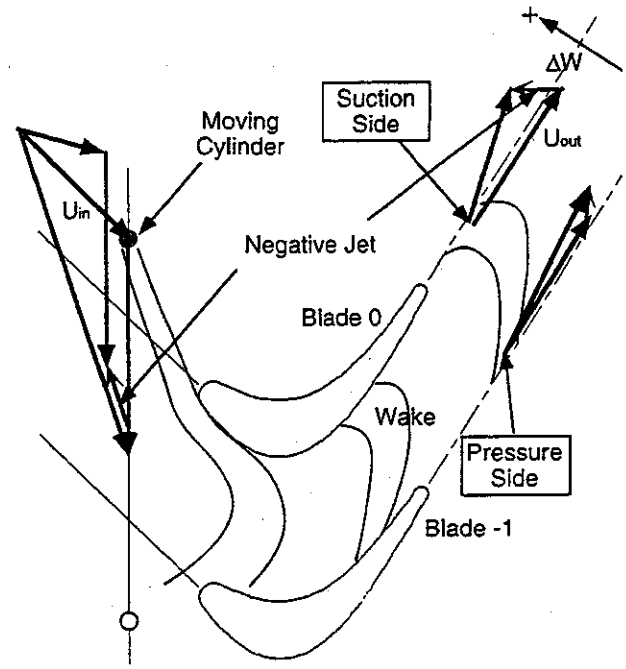

Figure 14 Schematic of the wake-blade interaction

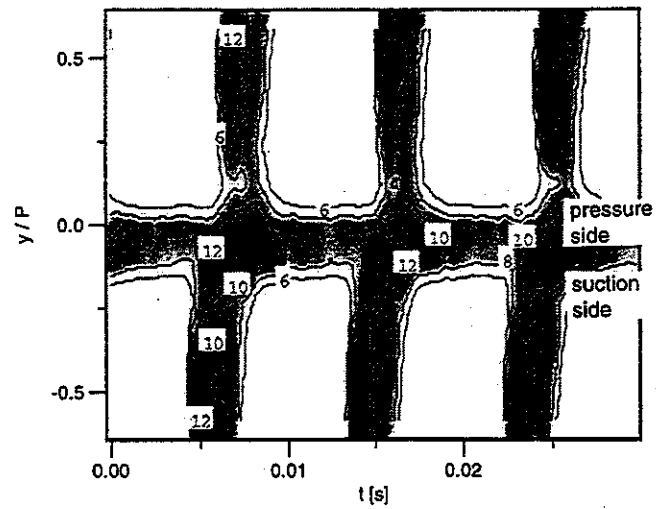

Figure 15 Contours of the time-resolved turbulence intensity on the distance-time diagram (blade midpan at Slot 1)

the negative jet of the wake as well as due to the wake deformation caused within the blade-to-blade passage, as schematically illustrated in Figure 14.

Figure 15 shows the contours of the *quasi* turbulence intensity on the distance-time diagram. Wake-associated turbulence intensity became small on the pressure side of the blade wake compared to that on the suction side. Such a tendency could be also identified at the downstream of Slot 1, although broadened blade wakes and the dissipation of the bar wakes made it undistinguished. High turbulence intensity regions periodically appeared inside the blade wake, which requires further investigation.

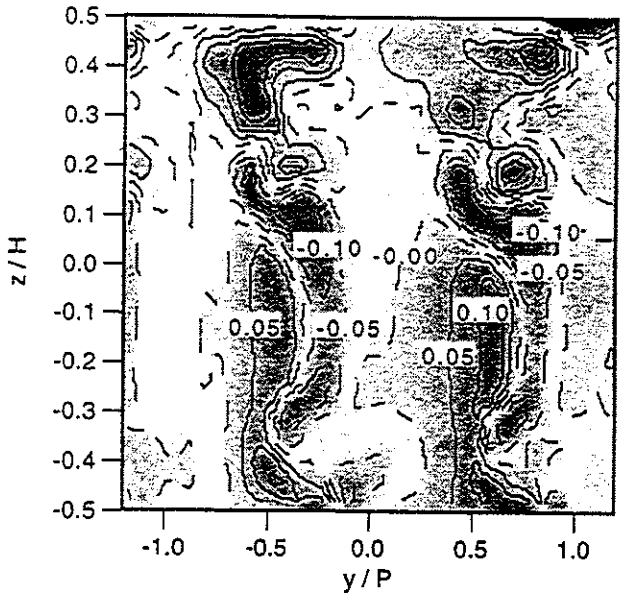

Figure 15 Difference in stagnation pressure loss between the cases with wakes and with no wakes at Slot 2 (+ : increase / - : decrease)

DISCUSSION

As mentioned above, the present definition measured the stagnation pressure loss by taking a difference between the pitchwise-averaged stagnation pressure at the inlet of the cascade and the local stagnation pressure downstream of the cascade. If incoming wakes had mixed out before the entrance of the cascade, the loss associated with the bar wakes would have been no longer identified at the downstream of the cascade. Actually, however, the incoming wakes did not mixed out even at the exit of the cascade, so that one could recognize the appearance of the stagnation pressure loss at Slot 1 as seen in Figures 7 and 8. It was found in Figure 15 that these high loss regions gradually shifted towards to the blade suction surface as the measuring location went downstream, although secondary flow effects made it difficult to draw a general conclusion. The effects of the so-called negative jet provide explanation to the observations that those high loss regions clustered near by the suction side. What the negative jet model, proposed by Kerrebrock and Mikolajczak (1970), suggests in the present case is that a fluid particle with relatively low stagnation pressure associated with the incoming wake drifted towards the suction side of the flow passage due to a resultant *slip* velocity inside the wake.

Another possible factor that caused the biased distributions of the stagnation pressure loss is a mixing loss between the low momentum fluid inside the wake and a relatively uniform main stream. Since the inlet flow fields was not fully mixed out downstream of the cascade as observed in the time-resolved yaw-angle of Figure 13, there still existed the considerable velocity difference between the center of the wake and the main stream. This, in conjunction with the negative jet effect, could contribute to the clustering of the stagnation pressure loss near the suction side of the blade wake. Flow acceleration /deceleration over the pressure or suction surface of the blade seemed to assist this tendency as pointed out by Denton (1993). Denton describes that velocity difference between the wake centerline and the mainstream decreases or increases due to the flow acceleration or deceleration. The flow over the suction surface experiences gradual deceleration from the throat to the trailing edge, while the flow over the pressure surface accelerates as it approaches the trailing edge. It appears that this theory supports the present observation of the stagnation pressure loss clustered near the suction side.

Recently, Curtis et al. (1996)[1] found similar clustered high loss regions near the *pressure side* of the blade wakes downstream of the LP turbine blades. This is in sharp contrast to the present case in which high loss regions appeared near the *suction side* of the blade wakes. Hosdon and Dawes (1996) presented an interpretation on these phenomena. Hodson and Dawes, citing the following relationship between the stagnation enthalpy h_0 and the static pressure p,

$$\frac{Dh_0}{Dt} = \frac{1}{\rho}\frac{\partial p}{\partial t}, \qquad (9)$$

concluded that a fluid over the suction surface tended to experience a more positive static pressure fluctuation $\partial p/\partial t$ than a negative value and this was the main reason for the lowered stagnation pressure loss (or increase in stagnation pressure) observed on the suction side of the blade wake. Their conclusion seems to be plausible at first glance. However, if the Eq. (9) dominates the non-uniformity of the wake-affected stagnation pressure at the cascade exit, high loss regions do not necessarily appears only on the pressure side of the blade wake, which is in contrast to the explanation by use of the negative jet model. Furthermore, Funazaki and Nishiyama (1989) found that profiles of wake-affected stagnation loss of a turbine cascade varied with the ratio of the bar pitch to the blade pitch, which was related to the bar-passing frequency as well as the inter-blade phase angle. In the numerical simulations done by Hodson and Dawes, the bar pitch/blade pitch ratio was 1.0, whereas the ratio was 0.667 in the related experiment done by Curtis et al. (1996). According to Funazaki and Nishiyama, this difference could affect the conclusion of Hodson and Dawes to some extent. Further parametric investigations, experimentally as well as numerically, are greatly needed on the effect of the static pressure fluctuation. Besides, the present authors feel that there coexist those two effects, i.e., the static pressure fluctuation and the negative jet, in the flow field concerned . It could be accordingly supposed that they promote the biased stagnation pressure loss distribution together in some cases and they cancel with each other in the other cases. This supposition will be checked in a future study.

CONCLUSIONS

In this study loss measurements were performed in the cascade of high pressure turbine blades under the influence of periodically passing wakes. Major findings in this study are listed as follows:

(1) From the pneumatic probe measurements, it was found that relatively high loss regions tended to cluster near the suction side of the blade wakes at the midspan.

(2) The stagnation pressure loss associated with the blade wake was generally reduced by the passage of the bar-wakes. Flow visualization revealed that this loss reduction was closely related to the suppression of the separation bubble on the blade suction surface due to the wake passage.

(3) Hot-wire probe measurements of the exit flow from the cascade at the blade midspan clearly verified the existence of the negative jet effect in terms of instantaneous variation of yaw angle and turbulence intensity.

(4) Some discussions were made on the mechanism of the non-

[1] In the paper of Cutris et al., no data on the loss profile were shown. Instead Hodson and Dawes (1996) presented those profiles.

uniform distribution of the stagnation pressure loss observed at the exit of the cascade. Negative jet effects seemed to play an important role in this phenomenon in the present study. However, the present results conflicted the experimental and numerical findings by the groups of Whittle Laboratory, Cambridge University. Therefore further investigations are required in order to clarify the wake effect upon the unsteady loss generation in the turbine rotor cascade.

ACKNOWLEDGMENT

The authors are greatly indebted to Mr. H. Nakayasu for his contribution in conducting the experiments.

REFERENCES

Bruun, H.H., 1975, "Interpretation of X-Hot-Wire Signals," DISA Information, Vol. 18, p. 5.

Curtis, E. M., Hodson, H. P., Banieghbal, J. D., Denton, J. D. and Howell, R. J., 1996, "Development of Blade Profiles for Low Pressure," ASME Paper 96-GT-358.

Denton, J. D., 1993, "Loss Mechanisms in Turbomachines," Trans. ASME Journal of Turbomachinery, Vol. 115, pp. 621 - 656.

Dring, R. P., Joslyn, H. D. and Blair, M. F., 1987, "The Effects of Inlet Turbulence and Rotor/Stator Interactions on the Aerodynamics and Heat Transfer of a Large-Scale Rotating Turbine Model," 179469, NASA Contractor Report 179469, p. 126.

Fujita, H. and Kovasznay, S. L. G., 1968, "Measurements of Reynolds Stress by a Single Rotated Hot Wire Anemometer," The Review of Science Intruments, Vol. 39, pp. 1351-1355.

Funazaki, K. and Nishiyama, T., 1989, "Measurements of Simulated Wake/Rotor Interaction Phenomena in Turbomachinery," Proceedings of Unsteady Aerodynamics and Aeroelasticity of Turbomachines and Propellers, Bejing, pp. 287-300

Funazaki, K., Yoyabu, E. and Yamawaki, S., 1996, "Effect of Periodic Wake Passing on Film Effectiveness of Inclined Cooling Holes around the Leading Edge of a Blunt Body," ASME Paper 96-GT-207.

Funazaki, K. and Tanuma, T., 1996, "Studies on Profile Loss Associated with Wake-Disturbed Unsteady Boundary Layer on a Flat Plate," Latest Advances in the Aerodynamics of Turbomachinery, IMechE Proceedings, S461/001

Gallus, H. E., 1991, "Experimental Methods and Results in Unsteady Aerodynamics and Aeroelasticity," Proccedings of Unsteady Aerodynamics, Aeroacoustics, and Aeroelasticity of Turbomachines and Propellers, University of Notre Dame, pp. 464-485.

Greitzer, E. M., 1985, "An Introduction to Unsteady Flow In Turbomachines," NATO ASI Series, Vol. 2, pp. 967-1024.

Halstead, D. E., Wisler, D. C., Okiishi, T. H., Walker, G. J., Hodson, H. P. and Shin, H. W., 1995, "Boundary Layer Development in Axial Compressor and Turbines, Part 4 of 4: Computations and Analysis," ASME Paper 95-GT-464.

Hodson, H. P. and Dawes, W. N., 1996, "On the Interpretation of Measured Profile Losses in Unsteady Wake-Turbine Interaction Studies," ASME Paper 96-GT-494.

Kerrebrock, J. L. and Mikolajczak, A. A., 1970, "Inter-Stator Transport of Rotor Wakes and Its Effect on Compressor Performance," Trans. ASME Journal of Engineering for Power, Vol. 92, pp. 359 - 370.

Ladwig, M. and Fottner, L., 1993, "Experimental Investigations of the Influence of Incoming wakes on the Losses of a Linear Turbine Cascade," ASME Paper 93-GT-394.

Matsubara, H., 1993, "Secondary Flows in a Model Cascade of a Steam Turbine," Master Thesis, Iwate University

Schlichting, H., 1979, "Boundary-Layer Theory," McGraw-Hill, p. 17.

Schulte, V. and Hodson, H. P., 1996, "Unsteady wake-Induced Boundary Layer Transition in High Lift Turbines," ASME Paper 96-GT-486.

Yamamoto, A., Kaba, K. and Matsunuma, T., 1994, "Unsteady Behaviors of Three-Dimensional Flows in Turbine Blade Passage-Part1:Experimental Work," Proceedings of Unsteady aerodynamics and Aeroelasticity of Turbomachines, Fukuoka, pp. 675-690

Yamamoto, A., Miura, F., Taminaga, J., Tomihira, S., Outa, E. and Matsuki, M., 1993, "Unsteady Three-Dimensional Flow Behavior due to Rotor-Stator Interaction in an Axial-Flow Turbine," ASME Paper 93-GT-404.